

# FEM investigation of leaky modes in hollow core photonic crystal bers

Jan Pomplun<sup>ab</sup>, Ronald Holzlohner<sup>c</sup>, Sven Burger<sup>ab</sup>, Lin Zschiedrich<sup>ab</sup>, Frank Schmidt<sup>ab</sup>,

<sup>a</sup> Zuse Institute Berlin, Takustra e 7, D { 14 195 Berlin, Germany

<sup>b</sup> JCM wave GmbH, Haarer Stra e 14a, D { 85 640 Putzbrunn, Germany

<sup>c</sup> European Southern Observatory, Karl-Schwarzschild-Stra e 2, D { 85 748 Garching, Germany,

Copyright 2007 Society of Photo-Optical Instrumentation Engineers.

This paper has been published in Proc. SPIE 6480, 6480-22 (2007), (Photonic Crystal Materials and Devices VI, A. Adibi, S.-Y. Lin, A. Scherer, Eds.) and is made available as an electronic reprint with permission of SPIE. One print or electronic copy may be made for personal use only. Systematic or multiple reproduction, distribution to multiple locations via electronic or other means, duplication of any material in this paper for a fee or for commercial purposes, or modification of the content of the paper are prohibited.

## ABSTRACT

Hollow-core holey bers are promising candidates for low-loss guidance of light in various applications, e.g., for the use in laser guide star adaptive optics systems in optical astronomy. We present an accurate and fast method for the computation of light modes in arbitrarily shaped waveguides. Maxwell's equations are discretized using vectorial finite elements (FEM). We discuss how we utilize concepts like adaptive grid refinement, higher-order finite elements, and transparent boundary conditions for the computation of leaky modes in photonic crystal bers. Further, we investigate the convergence behavior of our methods.

We employ our FEM solver to design hollow-core photonic crystal bers (HCPCF) whose cores are formed from 19 omitted cladding unit cells. We optimize the ber geometry for minimal attenuation using multidimensional optimization taking into account radiation loss (leaky modes).

**Keywords:** photonic crystal bers, simulation, FEM

## 1. INTRODUCTION

Photonic crystal bers (PCF) have a core surrounded by a periodic arrangement of holes and struts. This structure prevents leakage of light to the exterior.<sup>1</sup> In contrast to ordinary index-guiding optical bers the core can have a smaller refractive index than the surrounding material or even be hollow. Although hard to fabricate there are many application areas where the guidance principles of PCFs offer great advantages. An important example for the use of hollow-core photonic crystal bers (HCPCF) is the field of high-power light transmission,<sup>1</sup> e.g. for pulsed lasers for adaptive optics systems in astronomy.<sup>2</sup> Loss mechanisms of HCPCFs are coupling of the fundamental mode to interface modes due to diffuse scattering at glass/air interfaces and leakage of light to the exterior through the photonic crystal structure.<sup>2</sup> Another problem is the usually narrow transmission bandwidth.<sup>3</sup>

When producing a ber it is therefore very important to be able to optimize the ber design to match desired properties and minimize undesired losses. Because of the complicated structure of PCFs this can only be done numerically. The oldest approach for computation of modes in bers is the plane-wave expansion (PWE) method. Because of the complicated structure and great number of refractive index jumps in the ber cross section this method is inefficient. For example discontinuous behaviour of the propagation modes at the glass/air interfaces can only be described with a huge number of basis functions taken into account for computation. This leads to very large computation times and poor convergence behaviour of the method.<sup>2</sup> Moreover, the modeling of an infinite exterior and therefore the simulation of radiation leakage is very difficult with the PWE method. Here we present the finite-element method (FEM) for the computation of leaky modes in photonic crystal bers.

---

Corresponding author: J. Pomplun

URL: <http://www.zib.de/nano-optics/>

Email: pomplun@zib.de

## 2. FORMULATION OF THE PROPAGATION MODE PROBLEM

In this section we will derive the mathematical formulation of the propagation mode problem. The geometry of a fiber is invariant in one spacial dimension (along the fiber), here  $z$ -direction. A propagating mode is a solution to the time harmonic Maxwell's equations, which exhibits a harmonic dependency in  $z$ -direction:

$$\begin{aligned} E &= E_{pm}(x;y) \exp(ik_z z) \\ H &= H_{pm}(x;y) \exp(ik_z z) : \end{aligned} \quad (1)$$

$E_{pm}(x;y)$  and  $H_{pm}(x;y)$  are the electric and magnetic propagation modes and the parameter  $k_z$  is called propagation constant. If the permittivity and permeability can be written as:

$$\epsilon = \begin{pmatrix} \epsilon_{xx} & 0 \\ 0 & \epsilon_{zz} \end{pmatrix} \quad \text{and} \quad \mu = \begin{pmatrix} \mu_{xx} & 0 \\ 0 & \mu_{zz} \end{pmatrix} ; \quad (2)$$

we can split the propagation mode into a transversal and longitudinal component:

$$H_{pm}(x;y) = \begin{pmatrix} H_{\perp}(x;y) \\ H_z(x;y) \end{pmatrix} : \quad (3)$$

Inserting (1) with (2) and (3) into Maxwell's equations yields:

$$\begin{pmatrix} \epsilon_{xx} & 0 \\ 0 & \epsilon_{zz} \end{pmatrix} \begin{pmatrix} \nabla_{\perp}^2 H_{\perp} \\ \nabla_{\perp}^2 H_z \end{pmatrix} - \begin{pmatrix} \epsilon_{xx} & 0 \\ 0 & \epsilon_{zz} \end{pmatrix} \begin{pmatrix} \nabla_{\perp}^2 H_{\perp} \\ \nabla_{\perp}^2 H_z \end{pmatrix} - \begin{pmatrix} \epsilon_{xx} & 0 \\ 0 & \epsilon_{zz} \end{pmatrix} \begin{pmatrix} \nabla_{\perp}^2 H_{\perp} \\ \nabla_{\perp}^2 H_z \end{pmatrix} = \begin{pmatrix} \epsilon_{xx} & 0 \\ 0 & \epsilon_{zz} \end{pmatrix} \begin{pmatrix} H_{\perp} \\ H_z \end{pmatrix} ; \quad (4)$$

with

$$P = \begin{pmatrix} 0 & 1 \\ 1 & 0 \end{pmatrix} ; \quad r_{\perp} = \begin{pmatrix} \partial_x \\ \partial_y \end{pmatrix} : \quad (5)$$

Now we define  $H_z = k_z H_z$  and get:

$$\begin{pmatrix} \epsilon_{xx} & 0 \\ 0 & \epsilon_{zz} \end{pmatrix} \begin{pmatrix} \nabla_{\perp}^2 H_{\perp} \\ \nabla_{\perp}^2 H_z \end{pmatrix} - \begin{pmatrix} \epsilon_{xx} & 0 \\ 0 & \epsilon_{zz} \end{pmatrix} \begin{pmatrix} \nabla_{\perp}^2 H_{\perp} \\ \nabla_{\perp}^2 H_z \end{pmatrix} - \begin{pmatrix} \epsilon_{xx} & 0 \\ 0 & \epsilon_{zz} \end{pmatrix} \begin{pmatrix} \nabla_{\perp}^2 H_{\perp} \\ \nabla_{\perp}^2 H_z \end{pmatrix} = k_z^2 \begin{pmatrix} P & 0 \\ 0 & P \end{pmatrix} \begin{pmatrix} H_{\perp} \\ H_z \end{pmatrix} \times 2 R^2 : \quad (6)$$

Eq. (6) is a quadratic eigenvalue problem for the propagation constant  $k_z$  and propagation mode  $H_{pm}(x;y)$ . We get a similar equation for  $E_{pm}(x;y)$  exchanging  $\epsilon$  and  $\mu$ . For our numerical analysis we will not look at the propagation constant but define the effective refractive index  $n_e$  which we will also refer to as eigenvalue:

$$n_e = \frac{k_z}{k_0} \quad \text{with} \quad k_0 = \frac{2\pi}{\lambda_0} ; \quad (7)$$

where  $\lambda_0$  is the vacuum wavelength of light.

## 3. SOLUTION OF THE PROPAGATION MODE PROBLEM WITH THE FINITE-ELEMENT METHOD

In order to compute propagation modes we have to solve the eigenvalue problem (6) numerically. Note that this problem is formulated on  $R^2$ . We have an eigenvalue problem on an unbounded domain. Usually, propagation modes are computed on an artificially bounded domain applying either periodic or so called Dirichlet boundary conditions, i.e.  $E_{pm}(x;y) = 0$  for  $(x;y) \in \partial$  (propagation mode vanishes on the boundary  $\partial$  of the computational domain). Using this simplification it is not possible to model leaking of light from the core of the fiber to the exterior (leaky modes). Here we want to take this effect into account. Since our computational domain still has to be of finite size, we apply so-called transparent boundary conditions to  $\partial$ . We realize these boundary conditions with the perfectly matched layer (PML) method.<sup>4</sup> The propagation constant  $k_z$  becomes complex and the corresponding mode is damped according to  $\exp(-\text{Im}(k_z)z)$  while propagating along the fiber. This damping is due to radiation leakage from the fiber to the exterior.

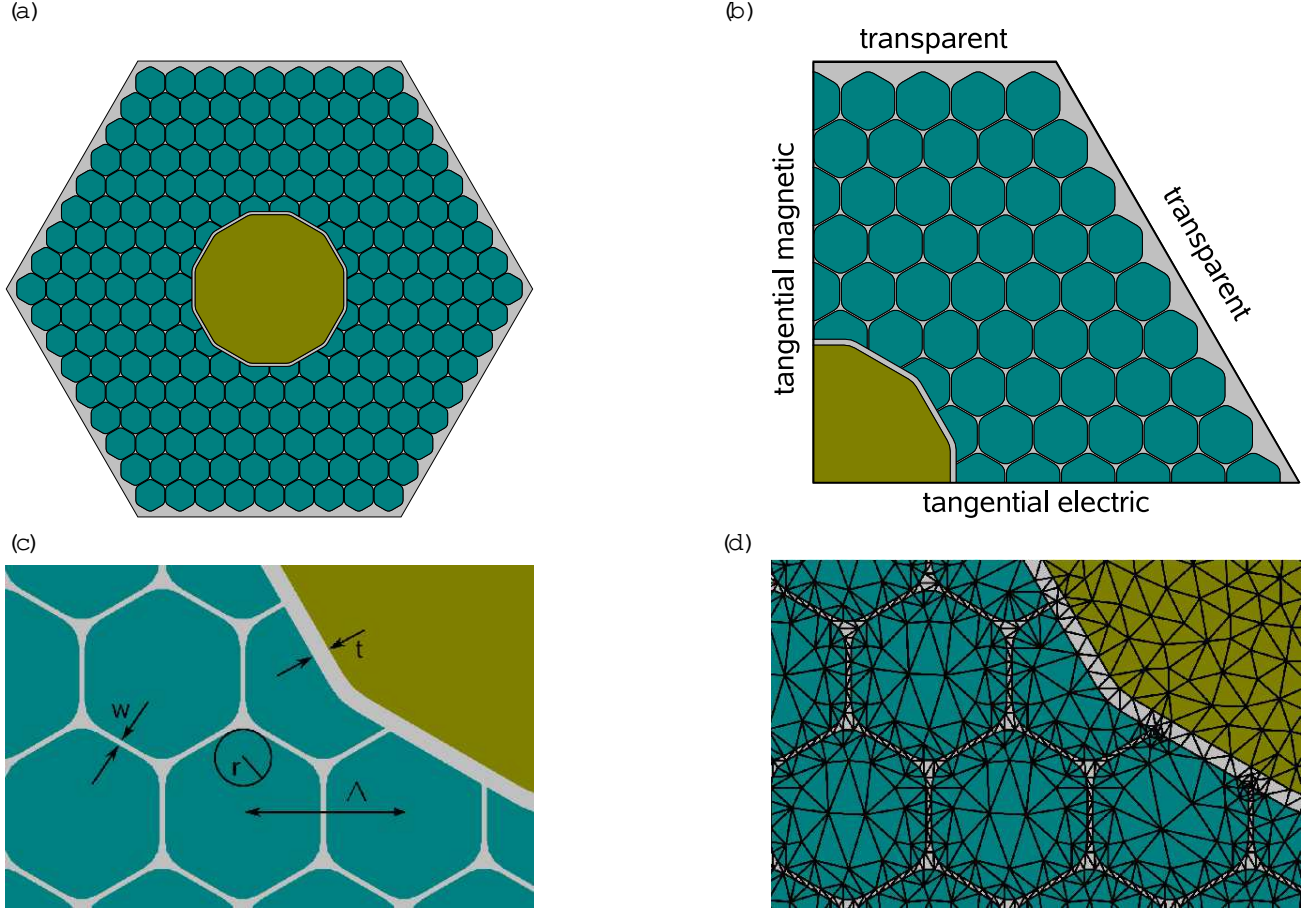


Figure 1. (a) Geometry of HCP CF used for mode computation; (b) boundary conditions for mode computation with a quarter of the fiber; (c) geometrical parameters describing HCP CF. Pitch  $\Lambda$ , hole edge radius  $r$ , strut thickness  $w$ , core surround thickness  $t$ ; (d) detail from a triangulation of HCP CF. Due to the flexibility of triangulations all geometrical features of the HCP CF are resolved.

In contrast to the PWE method, whose ansatz functions are spread over the whole computational domain (plane waves) the FEM method uses localized ansatz functions. To construct these ansatz functions, the computational domain has to be discretized. This means the geometry is subdivided into  $N$  patches, e.g. triangles in two dimensions, tetrahedra in three dimensions. Fig. 1 (d) shows such a triangulation of a photonic crystal fiber (Fig. 1 (c)). On the patches usually polynomial ansatz functions are defined. Since we are solving Maxwell's equations, our solution is a vectorial function and therefore we use vectorial ansatz functions  $\mathbf{h}_i(\mathbf{x};\mathbf{y})$ . The numerical solution for the electric field  $\mathbf{E}$  is a superposition of these localized ansatz functions

$$\mathbf{E}(\mathbf{x};\mathbf{y}) = \sum_{i=1}^N h_{i-1}(\mathbf{x};\mathbf{y}) \quad (8)$$

The FEM computation determines the unknown coefficients  $h_{i-1}$ . The FEM method has several advantages:

Maxwell's equations are solved rigorously without approximations.

The flexibility of triangulations allows the computation of virtually arbitrary structures without simplifications or approximations, as illustrated in Fig. 1 (d).

Choosing appropriate ansatz functions  $\mathbf{h}_i(\mathbf{x};\mathbf{y})$  for the solution of Maxwell's equations, physical properties of the electric field like discontinuities or singularities can be modeled very accurately and don't give rise

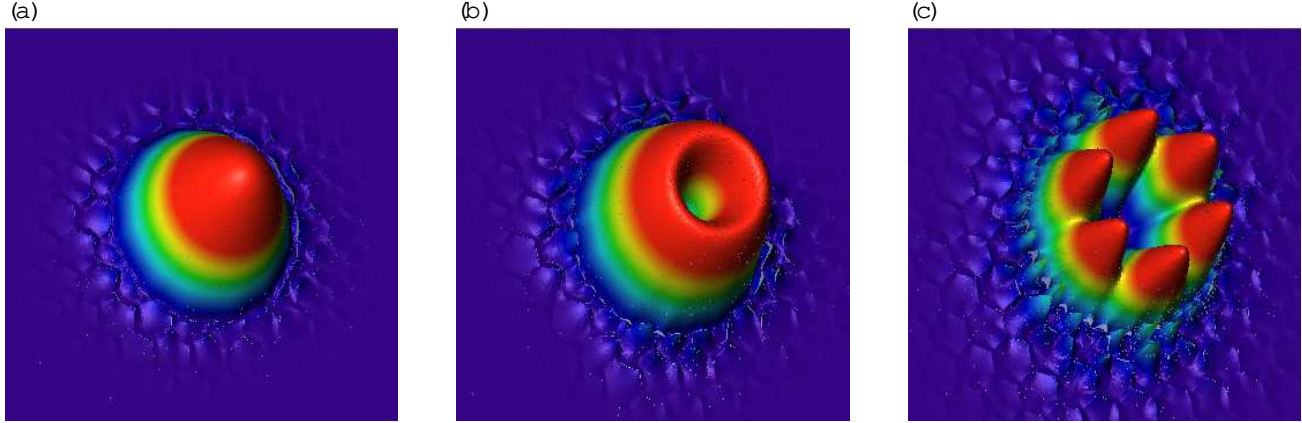


Figure 2. First, second and fourth fundamental core modes of HCPCF illustrated in Fig. 1 (a) - Parameters:  $\Lambda = 1550 \text{ nm}$ ,  $r = 300 \text{ nm}$ ,  $w = 50 \text{ nm}$ ,  $t = 170 \text{ nm}$ .

to numerical problems. Such discontinuities often appear at glass/air interfaces of photonic crystal fibers, see Fig. 2 (c).

Adaptive mesh-refinement strategies lead to very accurate results and small computational times which is a crucial point for optimization of fiber design.

The FEM approach converges with a fixed convergence rate towards the exact solution of Maxwell-type problems for decreasing mesh width (i.e. increasing number  $N$  of sub-patches) of the triangulation. Therefore, it is easy to check if numerical results can be trusted.<sup>5</sup>

In the following sections we apply the FEM method to the computation of leaky propagation modes in HCPCFs. The only simplification we make is to extend the fiber cladding to infinity and thereby neglect its finite size. This is justified if the cladding of the fiber is much larger than the microstructured core, and no light entering the cladding is reflected back into the core, which is usually the case.

Throughout this paper we use the FEM package JCM suite developed at the Zuse Institute Berlin for the numerical solution of Maxwell's equations. It has been successfully applied to a wide range of electromagnetic field computations including waveguide structures,<sup>6</sup> DUV phase masks,<sup>7</sup> and other nano-structured materials.<sup>8,9</sup> It provides higher-order edge elements, multi-grid methods, a-posteriori error control, adaptive mesh refinement, and adaptive transparent boundary conditions. Further numerical details about the computation of leaky modes with JCM suite can be found in.<sup>10</sup>

#### 4. NUMERICAL ASPECTS OF PROPAGATION MODE COMPUTATION

Fig. 2 shows the first, second, and fourth core modes with lowest energy of the HCPCF illustrated in Fig. 1 (a). All of these core modes appear several times in the spectrum because of the  $C_{6V}$  symmetry of the layout. To decrease the problem size, we only use one quarter of the fiber as computational domain. Of course we should obtain the same eigenvalues taking the full, half or quarter fiber as computational domain, as demonstrated in Table 1. The imaginary part of the eigenvalue is much smaller than the real part. The differences in  $\text{Im}(n_e)$  are therefore due to the numerical uncertainty at the chosen refinement level.  $\text{Im}(n_e)$  will of course converge with increasing number of ansatz functions, see Fig. 3. Figure 1 (b) shows which boundary conditions we apply to the artificial inner boundaries for the case of a quarter fiber. These boundary conditions follow from symmetry of the core modes. Note that the imaginary and real parts of the eigenvalues differ by 11 orders of magnitude. Computation of leaky modes is therefore a multi-scale problem which makes it numerically very difficult. When analyzing radiation losses of a fiber, the imaginary part of the effective refractive index  $n_e$  is the quantity of interest. In the following we analyze how accurately we can compute  $n_e$ , i.e. we look at the convergence of the FEM computation. Therefore we compute  $n_e$  with an increasing number of unknowns. We can either refine

	unknowns	1st eigenvalue	2nd eigenvalue	3rd eigenvalue
full ber	861289	0.998265726 + 9.508 $10^{12}i$	0.99212759 + 1.513 $10^{10}i$	0.9908968 + 2.089 $10^{10}i$
half ber	438297	0.998265719 + 9.357 $10^{12}i$	0.99212742 + 1.489 $10^{10}i$	0.9908958 + 2.086 $10^{10}i$
quarter ber	218504	0.998265724 + 9.372 $10^{12}i$	0.99212652 + 1.504 $10^{10}i$	0.9909169 + 2.302 $10^{10}i$

Table 1. First, second and third eigenvalue computed with full, half and quarter ber as computational domain.

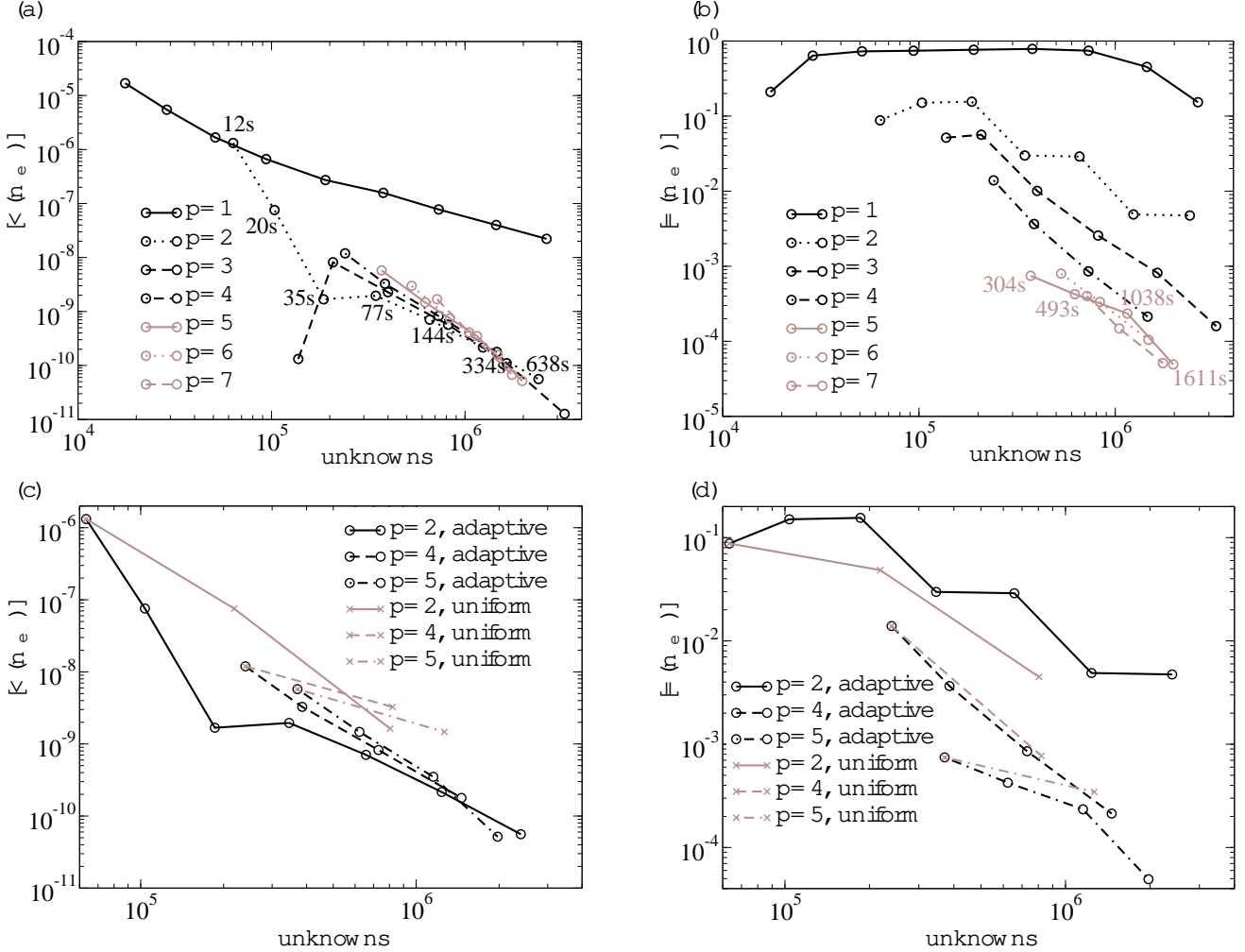


Figure 3. Relative error of first eigenmode in dependence on number of unknowns of FEM computation for different FEM degrees  $p$ . (a) and (b): adaptive refinement; (c) and (d) comparison of adaptive and uniform refinement. Parameters:  $\lambda = 1550 \text{ nm}$ ,  $r = 300 \text{ nm}$ ,  $w = 50 \text{ nm}$ ,  $t = 170 \text{ nm}$ .

the triangulation or increase the polynomial degree  $p$  of the ansatz functions on each patch to obtain a more accurate numerical result. The software package JCM suite offers finite elements with a maximum degree of 9. Furthermore, the refinement of the grid can be performed uniformly or adaptively. In a uniform refinement step each triangle is subdivided into 4 smaller ones. In an adaptive refinement step, an a-posteriori error estimator automatically chooses a certain number of triangles where the error of the FEM solution is large. Only these triangles are refined. This method leads to accurate results with smaller number of unknowns which also implies shorter computational times and smaller memory requirements. Fig. 3 shows the relative error of the real and imaginary parts of  $n_e$  in dependence on the number of unknowns of the FEM computation for different FEM degrees  $p$ . The relative error decreases with an increasing number of unknowns. Let us first look at the

convergence with adaptive refinement 3(a), (b). For the real part we achieve the fastest convergence for a finite element degree of 2. Note that already for a finite element degree of 1 and only 20;000 unknowns we have a relative error smaller than  $10^{-5}$ . For  $10^6$  unknowns we have a relative error smaller than  $10^{-9}$  for FEM degrees greater than 1. The imaginary part of the effective refractive index is much harder to compute accurately. For the same number of unknowns its relative error is much larger than the relative error of the real part. For a FEM degree of 1 the imaginary part does not converge at all up to  $3 \cdot 10^6$  unknowns. However the higher the FEM degree the faster the imaginary part converges. For the computation of leaky modes in HCPCFs it is therefore important to employ higher-order finite elements. Fig. 3(c), (d) shows a comparison of the convergence of the real and imaginary parts between adaptive and uniform refinement. While adaptive refinement leads to a faster convergence of the real part for all FEM degrees the imaginary part converges almost equally fast for an FEM degree of 4 and even slower for an FEM degree of 2. This happens because the imaginary part of the eigenvalue is much smaller than the real part. The error estimator which chooses triangles in the case of adaptive refinement primarily reduces the error of the real part first, since its contribution to the relative error of the complex eigenvalue is much larger than the imaginary part. Computing leaky modes a uniform refinement strategy is therefore more suitable if one is interested in the imaginary part and radiation losses.

For further numerical analysis of radiation losses of the HCPCF we choose a finite element degree of 6 and no refinement step. With these settings the numerical problem has approximately 500;000 unknowns for a triangulation according to Fig. 1(d). The relative error of the real and imaginary parts is  $10^{-8}$  and  $10^{-3}$  respectively, according to the convergence curves. Such a computation requires 2GB RAM and about 10 minutes computation time on a standard desktop PC. It is fast enough for multidimensional optimization of the fiber design.

## 5. OPTIMIZATION OF HCPCF DESIGN

In this section we want to optimize the fiber design shown in figure 1(a) in order to reduce radiation losses, i.e. we want to minimize  $\text{Im}(n_e)$ . The basic fiber layout is a 19-cell core with rings of hexagonal cladding cells. Since these cladding rings prevent leakage of radiation to the exterior we expect that an increasing number of cladding rings reduces radiation leakage and therefore  $\text{Im}(n_e)$ . This is confirmed by our numerical simulations shown in Fig. 4. The radiation leakage decreases exponentially with the number of cladding rings and thereby the thickness of the photonic crystal structure. This behavior agrees with the exponential damping of light propagating through a photonic crystal structure with frequency in the photonic band gap.

For our further analysis we fix the number of cladding rings to 6. The free geometrical parameters are the pitch  $\Lambda$ , hole edge radius  $r$ , strut thickness  $w$ , and core surround thickness  $t$ , see Fig. 1(c). Fig. 4 shows the imaginary part of the effective refractive index in dependence on these parameters. For each scan all but one parameter were fixed. For the strut thickness  $w$  and the hole edge radius  $r$  we find well-defined optimal values which minimize  $\text{Im}(n_e)$ . For pitch  $\Lambda$  and core surround thickness  $t$  a large number of local minima and maxima can be seen. Now we want to optimize the fiber design using multidimensional optimization with the Nelder-Mead simplex method.<sup>2</sup> To reduce the number of optimization parameters we fix the hole edge radius to the determined minimum at  $r = 354 \text{ nm}$  since its variation has the smallest effect on  $\text{Im}(n_e)$ . For optimization we have to choose starting values for  $\Lambda$ ,  $t$  and  $w$ . Since the simplex method searches for local minima we have to decide in which local minimum of  $\Lambda$  and  $t$  we want to search. We choose  $t = 152 \text{ nm}$  since here  $\text{Im}(n_e)$  has a global minimum and  $\Lambda = 1550 \text{ nm}$  since the bandwidth of this minimum is much larger than for the global minimum at  $\Lambda = 1700 \text{ nm}$ .

Optimization yields a minimum value of  $\text{Im}(n_e) = 5 \cdot 10^{-15} \frac{1}{\text{m}}$  for the imaginary part of the effective refractive index. The corresponding geometrical parameters are  $\Lambda = 1597 \text{ nm}$ ,  $w = 38 \text{ nm}$ ,  $t = 151 \text{ nm}$ .

## 6. CONCLUSION

We have demonstrated that the finite element method is very well suited for the analysis of light propagation in hollow-core photonic crystal fibers. Here we considered a 19-cell HCPCF with 6 cladding rings. A convergence analysis allowed us to quantify the relative error of real and imaginary parts of the propagation constant of leaky eigenmodes. The real part could be computed in 20s on a standard desktop PC down to a relative error of

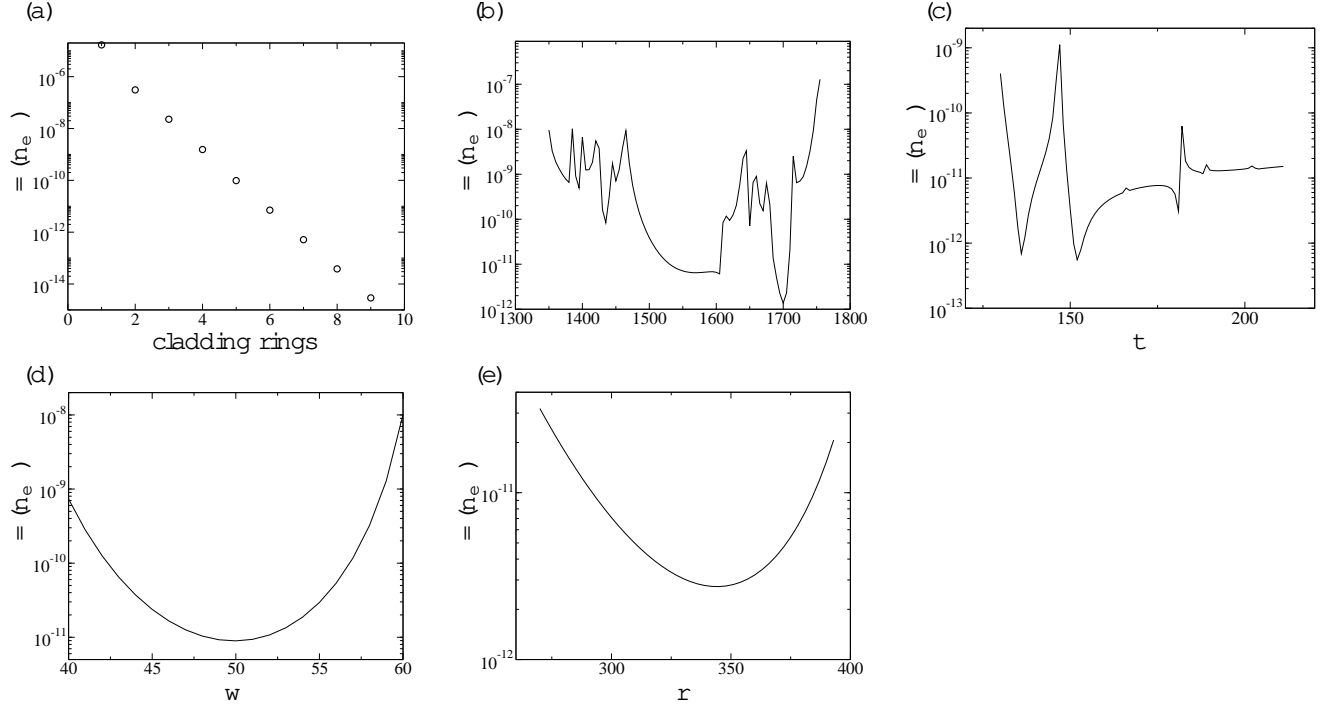


Figure 4. Imaginary part of the effective refractive index  $= \text{Im}(n_e)$  in dependence on: (a) number of cladding rings, (b) pitch  $p$ , (c) core surround thickness  $t$ , (d) strut thickness  $w$ , (e) hole edge radius  $r$ . Parameters:  $p = 1550$  nm,  $r = 300$  nm,  $w = 50$  nm,  $t = 170$  nm, 6 cladding rings, wavelength  $\lambda = 589$  nm.

$10^{-7}$ . The imaginary part, being 10 orders of magnitude smaller, could be determined in about 10 min with a relative error smaller than  $10^{-3}$ . Thanks to the short computational time, we were able to optimize the fiber design regarding pitch, strut thickness, core surround thickness, and hole edge radius of the cladding cells and thereby minimize radiation losses.

## 7. ACKNOWLEDGEMENT

We acknowledge support by DFG within SP 1113. Furthermore we thank P.J. Roberts for fruitful discussions.

## REFERENCES

1. P. Russell, "Photonic crystal fibers," *Science* 299 (5605), pp. 358{362, 2003.
2. R. Holzlohner, S. Burger, P. J. Roberts, and J. Pomplun, "Efficient optimization of hollow-core photonic crystal fiber design using the finite-element method," *JEO S* 1 (06011), 2006.
3. F. Couny, F. Benabid, and P. Light, "Large-pitch kagome structured hollow-core photonic crystal fiber," *Optics Letters* 31 (24), pp. 3574{3576, 2006.
4. J. Berenger, "A perfectly matched layer for the absorption of electromagnetic waves," *J. Comput. Phys.* 114 (2), pp. 185{200, 1994.
5. P. Monk, *Finite Element Methods for Maxwell's Equations*, Oxford University Press, 2003.
6. S. Burger, R. Köhler, A. Schädle, and F. S. and L. Zschiedrich, "FEM modelling of 3d photonic crystals and photonic crystal waveguides," in *Integrated Optics: Devices, Materials, and Technologies IX*, Y. Sidorin and C. A. W. Achter, eds., 5728, pp. 164{173, Proc. SPIE, 2005.
7. S. Burger, R. Köhler, L. Zschiedrich, W. Gao, F. Schmidt, R. März, and C. Nölcher, "Benchmark of FEM, waveguide and FDTD algorithms for rigorous mask simulation," in *Photomask Technology*, J. T. Weed and P. M. Martin, eds., 5992, pp. 378{389, Proc. SPIE, 2005.

8. C. Enkrich, M. Wegener, S. Linden, S. Burger, L. Zschiedrich, F. Schmidt, C. Zhou, T. Koschny, and C. M. Soukoulis, "Magnetic metamaterials at telecommunication and visible frequencies," *Phys. Rev. Lett.* 95, p. 203901, 2005.
9. T. Kalkbrenner, U. H. Kanson, A. Schadle, S. Burger, C. Henkel, and V. Sandoghdar, "Optical microscopy using the spectral modulations of a nano-antenna," *Phys. Rev. Lett.* 95, p. 200801, 2005.
10. L. Zschiedrich, S. Burger, R. Klose, A. Schadle, and F. Schmidt, "JCM mode: an adaptive finite element solver for the computation of leaky modes," in *Integrated Optics: Devices, Materials, and Technologies IX*, Y. Sidorin and C. A. Wachter, eds., 5728, pp. 192-202, Proc. SPIE, 2005.